Land Surface Emissivity in the GSI: Evaluation of the First Guess and Quality Control

Biljana Orescanin[1], B. Johnson[2], A. Collard[3] and T. Auligne[4]

1: RTi @ NOAA/STAR/JCSDA; 2: UCAR @ NOAA / JCSDA, formerly AER @ NOAA / JCSDA ; 3: IMSG @ NOAA/EMC; 4: NOAA/JCSDA

Contact Information: Biljana.Orescanin@noaa.gov

Objectives

Key goal for this recent effort supported by JCSDA:
In order to assess the land emissivity data quality, improve the quantity of assimilated radiances over land, and to better assimilate surface-sensitive channels over non-ocean surfaces we start this work with the goal of improving the emissivity first guess within the Gridpoint Statistical Interpolation (GSI) system.

A lack of emissivity observation data on the global scale is one of many difficulties for emissivity retrievals. Most of the field campaigns for land emissivity studies are short-lived and of small scale, and generally are not carried out in coordination with any specific satellite-based instruments or overpasses. This study focuses on testing and implementing the emissivity to the GSI as a control variable using MW channels over land surfaces. Land surface emissivity for global scales are currently mostly derived from satellite-based observations though radiative transfer calculations. Over land surfaces the emissivity is especially important for simulating surface-sensitive channels due to its high spatial and temporal variability. Estimating the atmospheric contribution from cloudy or rainy atmosphere, as well as the strong atmospheric scattering and absorption of land surface signals under such conditions, is still seen as a challenge, especially at higher frequencies. The estimation of satellite radiance is a key component of assimilating satellite data into numerical weather prediction (NWP) models. In addition, surface emissivity is crucial for estimating surface temperature from satellite measurements, retrieval of atmospheric moisture and temperature profiles from satellites, and studies of the Earth's surface-atmosphere system such as surface energy balance and climate modeling.

Data and Methodology

TELSEM (Tool to Estimate Land Surface Emissivities at Microwave frequencies) atlas is a monthly-mean climatology of emissivities calculated from SSM/I observations at SSM/I frequencies (19, 22, 37 and 85 GHz for vertical and horizontal polarizations, except for 22 GHz which is vertical only), with a spatial resolution of 0.25°x0.25° at the equator (equal area grid). This climatology has been computed by averaging 8 years of SSM/I monthly-mean emissivities (from 1993 to 2000).
MIIDAPS (Multi-Instruments Integrated QC & Data Assimilation Pre-processing System) developed at JCSDA is the 1DVAR preprocessor based on MiRS (Microwave integrated Retrieval System) technology extended to hyper-spectral IR sensors.
CRTM is calculating its land emissivity. That is done in "Two Stream Solution" subroutine.
TELSEM and MIIDAPS are chosen as possible choices for the GSI's emissivity first guess. The two are compared against CRTM's emissivity in order to estimate their potential in this application using 4 window ATMS channels (24GHz, 31GHz, 50GHz, 52GHz) that are sensitive to surface properties.
NOTE: Results are shown only for channel 3 (50GHz V).

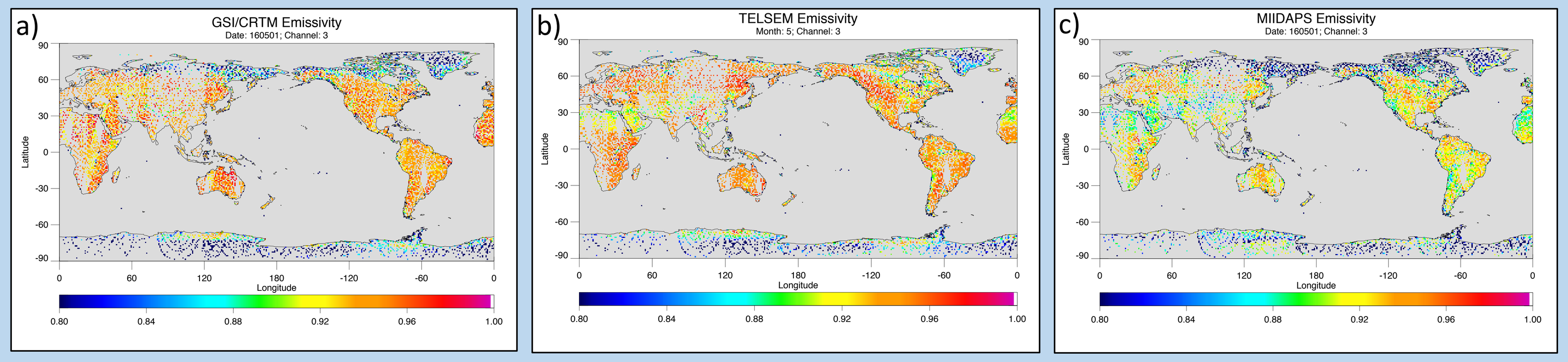

Fig.1 Emissivity map for AMTS sensor at 50 GHz channel for May 1st 2016 overpasses given by CRTM (a), TELSEM (b), and MIIDAPS (c). Note: TELSEM map shows emissivity for month of May

Emissivity maps suggest that CRTM does not reveal any features of the surface. E.g. there is no evidence of large features such as African desert? At the same time, both TELSEM and MIIDAPS show variability that reveals the land features. To better understand trends of the differences seen in Fig. 1, a surface type map with 14 surface classes is introduced.

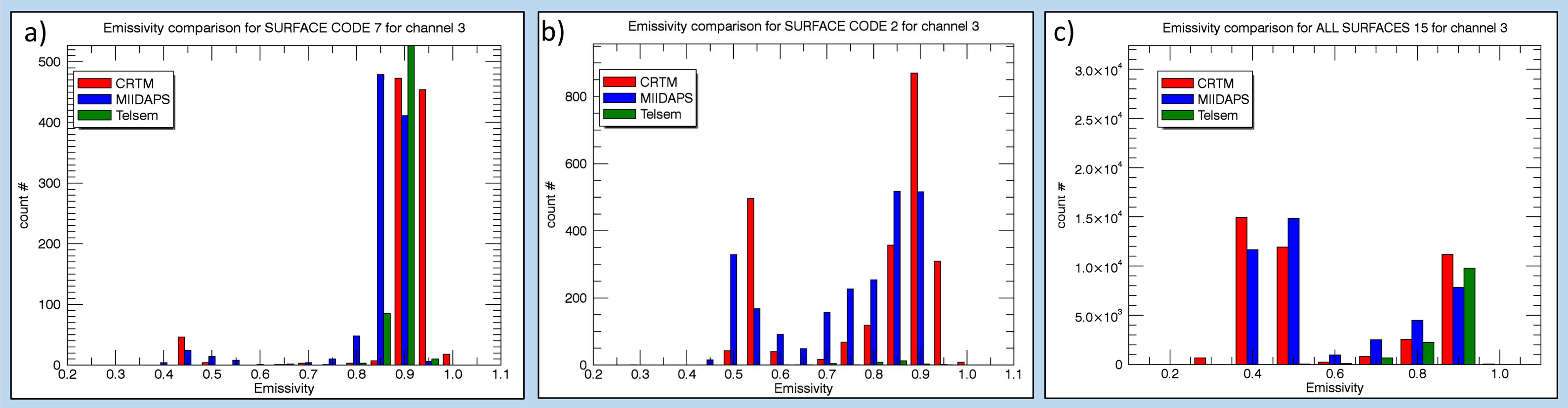

Fig.2 Histograms of surface emissivity given by CRTM, MIIDAPS, and TELSEM at ATMS channel 3 for : a) arid regions, b) areas of sea-ice, and c) all surfaces.

Surface-type-focused emissivity histograms shown in Fig 2. are based on TELSEM surface map with 14 surface classes. TELSEM emissivity for arid areas favors a single value (0.90) compared to the other two models. Further comparison of CRTM and MIIDAPS emissivity suggests that CRTM may have emissivity values that are too high (Fig. 2a and Fig. 3a-3b). One explanation of why deserts are not captured well by CRTM may be found in the lack of use of emissivity over this surface type, since satellite data is rarely used over arid/desert regions (e.g., W. CONUS and N. Africa) in GSI/CRTM model. For the sea-ice regions Fig 2b shows tendency of CRTM to group its emissivity values over high (0.90) and low (0.55) limits, suggesting that CRTM has less ability to depict transitions between ice-free sea surfaces and those that are fully covered with ice.

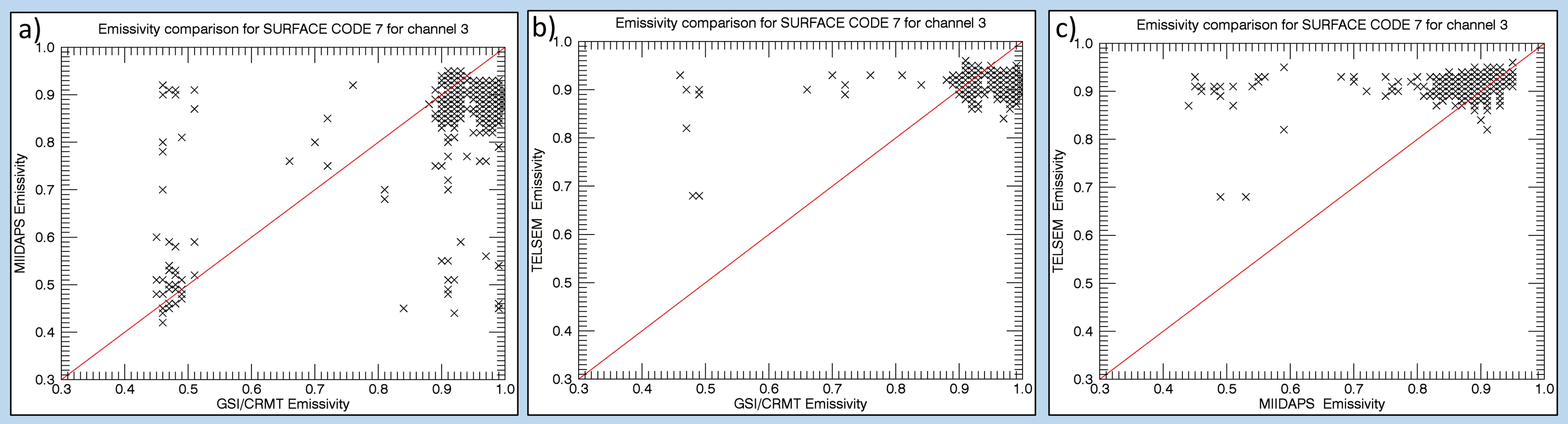

Fig.3 Emissivity comparison for arid areas for ATMS channel 3. a) GSI/CRTM vs. MIIDAPS; b) GSI/CRTM vs. TELSEM; c) MIIDAPS vs. TELSEM

To further investigate how the three models compare against each other scatter plots for arid areas (surface code 7, channel 3) are shown in Fig. 3. Here it is noticeable that CRTM is overestimating both TELSEM and MIIDAPS, when MIIDAPS and TELSEM are compared against each other the overestimation is seen on TELSEM side.

Based on comparisons of emissivity across all ATMS channels the study is continued by implementing both MIIDAPS and TELSEM emissivity into GSI system, as a first guess choice through two separate experiments that employ CRTM's user emissivity option to read in the data. This allowed for estimates of the first guess departures and more direct analysis of the potential that both models have in contribution towards better assimilation of emissivity data. The experiments were initialized with 1st May 2015 00Z initial conditions and ran till 3rd May 2015 00Z

Results

TELSEM First Guess Departures:

TELSEM - Indicates runs where TELSEM emissivity is used as user emissivity input option in CRTM, meaning climatological values are given to GSI as a first guess.
CRTM - Indicates runs where GSI employs emissivity calculated through CRTM using two-stream solution subroutine.

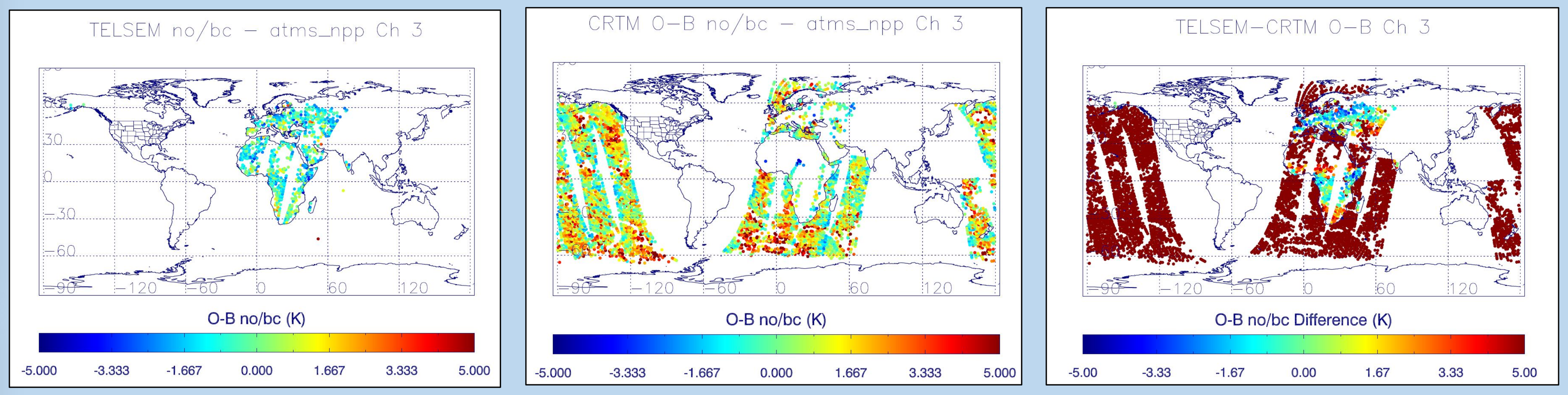

Fig. 4 First Guess Departures for TELSEM

MIIDAPS First Guess Departures:

MIIDAPS - Indicates runs where MIIDAPS is used as user emissivity input in CRTM, meaning 1DVAR emissivities are used as a first guess (i.e., dynamical emissivity)
CRTM – Indicates runs where GSI uses emissivity calculated through CRTM using the two-stream solution subroutine.

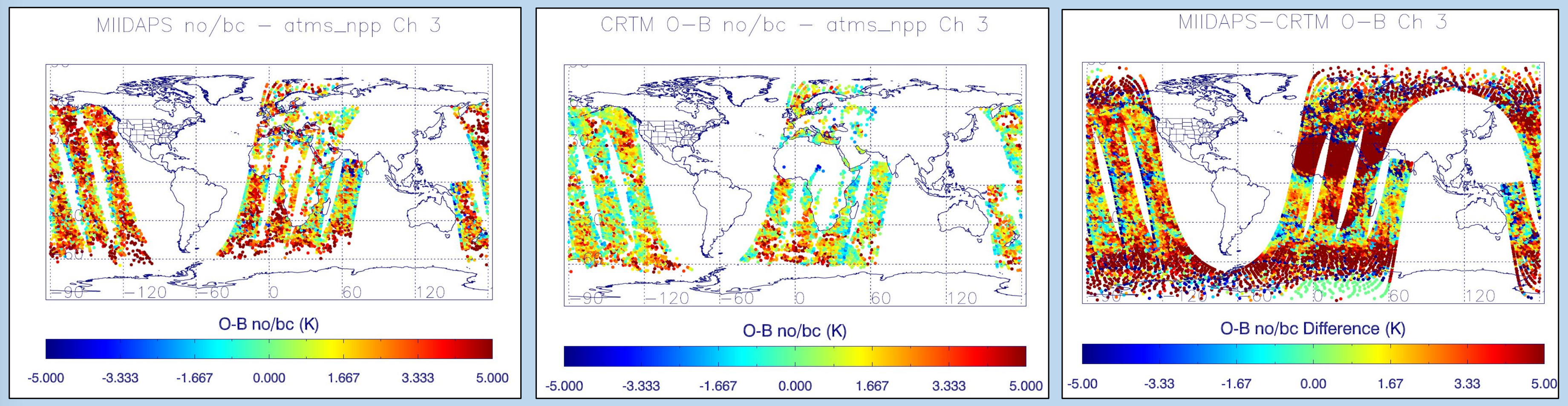

Fig. 5 First Guess Departures for MIIDAPS

The most striking feature in Fig. 4 is the difference between the two runs seen in the panel c) over the oceans (values greater than 5K). However, this is simply a consequence of the fact that TELSEM does not provide any data over the ocean. On the other side, by focusing on land surface only, one can note that the amount of data points brought to the GSI via TELSEM is significantly greater compared to CRTM case. Different physical features are clearly visible over land in TELSEM run. The same general trend is seen thorough all land-sensitive channels (1 through 4) of the ATMS instrument. Channels 16 and 17 have shown some sensitivity to the surface emissivity as well (not shown here).
When compared to Fig. 4, Fig. 5 suggests that MIIDAPS, in comparison to TELSEM, shows more noise while introducing fewer new data points.

1 cycle O-B	CRTM	MIIDAPS	TELSEM
Num. of Obs.	140	564	755
1 cycle O-A	**CRTM**	**MIIDAPS**	**TELSEM**
Num. of Obs.	167	1027	1062

Table. 1 Number of observations used in assimilation for first guess departures for TELSEM and MIIDAPS runs for one cycle of data.

Analysis of Quality Control (QC) and new QC implementation:

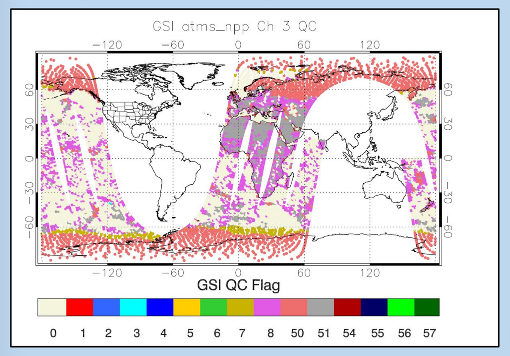

Figure 6 depicts data rejected due to invalid emissivities values and cloudy regions.
How to increase number of assimilated observation points?
- Defining better QC with new emissivity
- Introducing MIIDAPS CLW to screen out cloudy regions

Results for application in TELSEM and Control run are given in Fig.7

Fig. 6 Original QC done on data (flag 8 - rejection due to invalid emissivity)

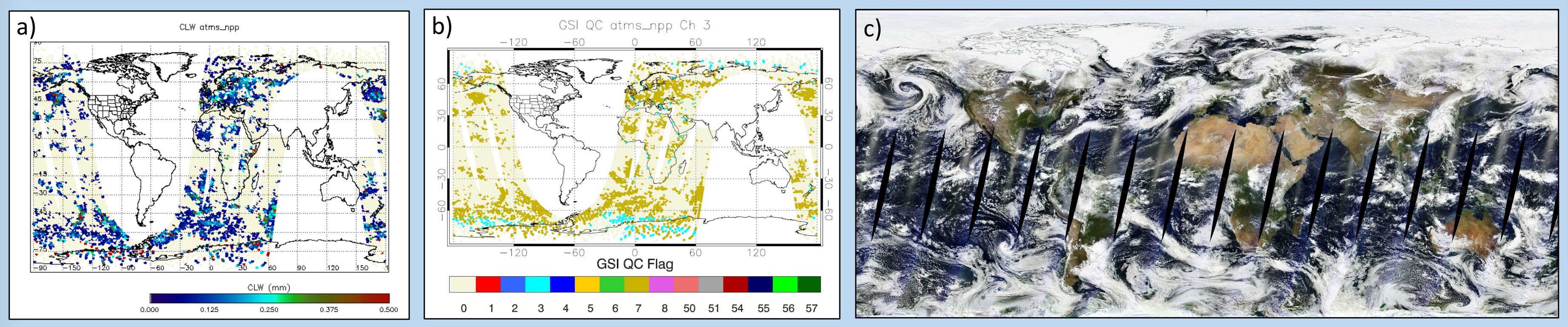

Fig. 7a CLW from MIIDAPS.; 7b New QC made out of MIIDAS data; 7c Terra Modis true color for 2015 05 02 (source: NASA Worldview)

First Guess Departures with new QC:

Based on these results, the best properties of the two models are combined and additional experiment is performed using TELSEM as a first guess and MIIDAPS as a QC. Analysis are shown in Fig.8

1 cycle O-B	TELSEM new QC
Num. of Obs.	1101
1 cycle O-A	**TELSEM new QC**
Num. of Obs.	1106

How does the new experiment run compare to the previous in respect to observation count? For both Observation minus Background (O-B) and Observation minus Analysis (O-A) the new observation count is increased compared to the Table 1.

Table 2. Number of observations for O-B and O-A TELSEM with new QC run for one cycle.

Results are based on 5 experiments comparing first guess departures and emissivity:
1. **Cntrl run with original QC** (CRTM calculated emissivities with operational QC)
2. **TELSEM with original QC** (TELSEM emissivity used as input to CRTM with operational QC)
3. **MIIDAPS with original QC** (MIIDAPS emissivity used as input to CRTM with operational QC)
4. **Cntrl with new QC** (CRTM calculated emissivities with QC cloud screening made out of MIIDAPS)
5. **TELSEM with new QC** (TELSEM for emissivity input with QC cloud screening made out of MIIDAPS)

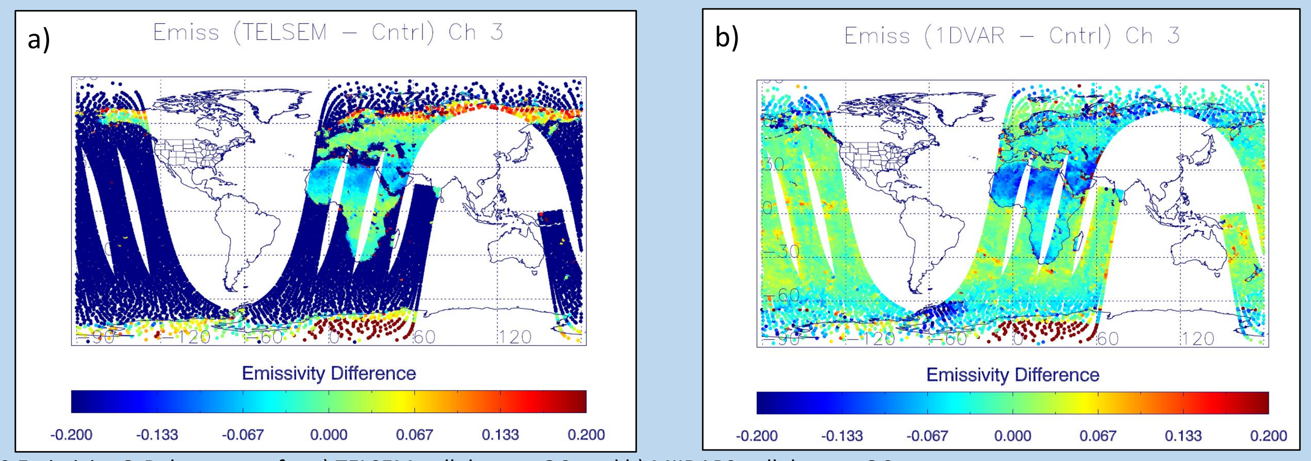

Fig. 9 Emissivity O-B departures for a) TELSEM - all data no QC, and b) MIIDAPS - all data no QC

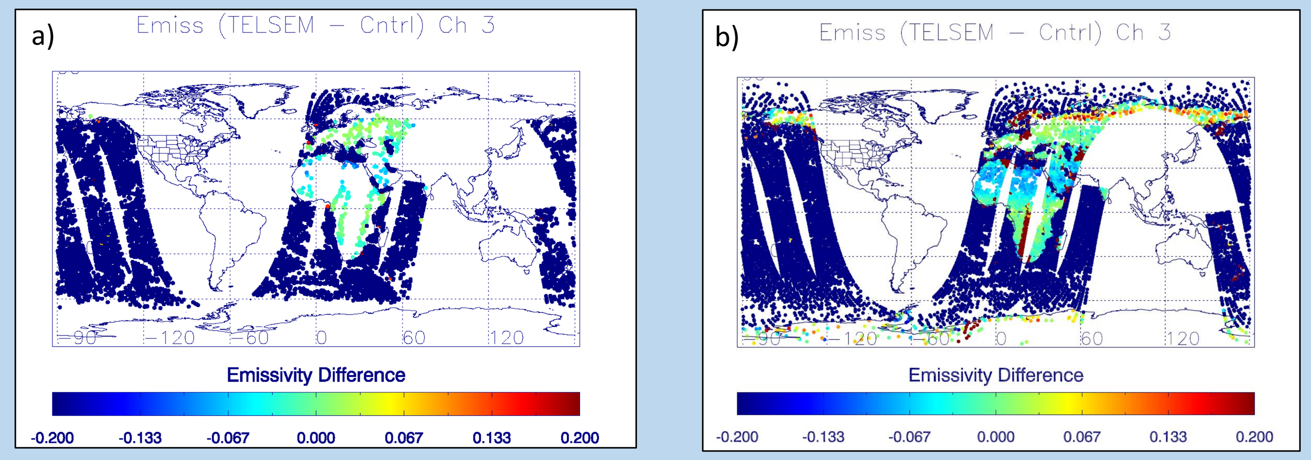

Fig. 10 Emissivity O-B departure for a) TELSEM - *experiment 2*, and b) Emissivity O-B for TELSEM with new QC - *experiment 5*

Emissivity departures maps:

Emissivity differences maps for both MIIDAPS and TELSEM without any quality control are shown in Fig. 9. Both maps reveal features that are not present in control run. Upon applying QC filtering, number of observations is reduced (see Fig. 10). However, significant differences exist between two QC criteria. In Fig. 10a majority of over land observations is removed, while the new QC filter (Fig. 10b) still preserves main emissivity features.

Fit to the Radiosonde Observations:

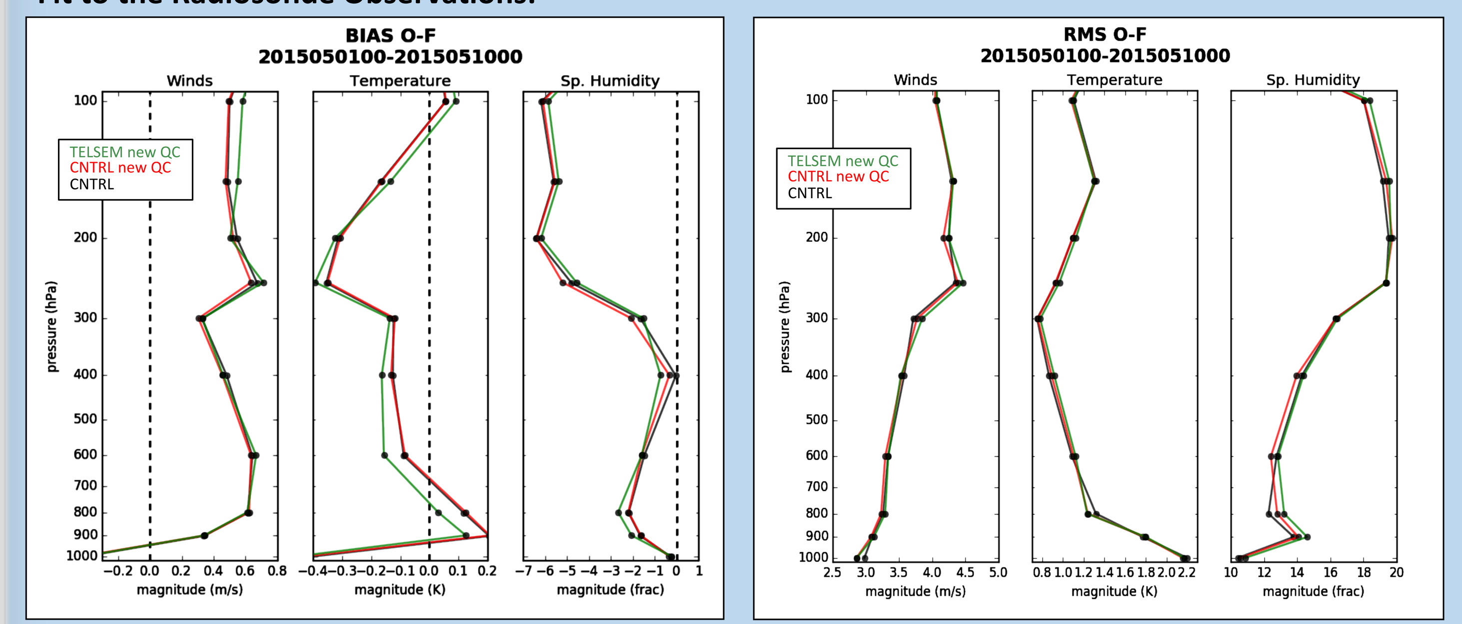

Fig. 11 Fit to radiosonde observations: BIAS (left) and RMS (right) comparison.

Further assessment of the wind, temperature and sp. humidity was performed by verifying against the radiosonde observations. Figure 11 shows the vertical profile of the temperature bias for 3 experiments (exp. 1 ,4 and 5) as one with most difference.

Conclusions

- Use of MIIDAPS dynamical emissivity and TELSEM emissivity climatology over land in place of physical model emissivity has shown increase in assimilated number of observations.
- Longer cycling is required to adjust bias correction coefficients before assessing impact on O-A and forecasts.
- Use of NEW QC, based on MIIDAPS retrieved CLW data, has also increased the number of assimilated observation.
- At the moment, the best results in respect to detection of land features are gained by using TELSEM as a first guess for emissivity in combination with MIIDAPS-based QC for cloud detection.
- Fit to radiosonde observations of wind, temperature and specific humidity indicates that more constraints on TELSEM with new QC is necessity in order to reduce current BIAS values.
- Control run with new QC gives us significantly better results with no adjustment needed.

Future Work

1. Create a longer run for validation of the methodology
2. Apply methodology to all sensors
3. Perform more detail analysis for results related to sea-ice
4. Implement emissivity as a control variable to GSI

References

- TELSEM: Aires, F., Prigent, C., Bernardo, F., Jiménez, C., Saunders, R. and Brunel, P. (2011), A Tool to Estimate Land-Surface Emissivities at Microwave frequencies (TELSEM) for use in numerical weather prediction. Q.J.R. Meteorol. Soc., 137: 690–699. doi:10.1002/qj.803
- MIIDAPS: Boukabara, S.-A., K. Garrett, W. Chen, F. Iturbide-Sanchez, C. Grassotti, C. Kongoli, R. Chen, Q. Liu, B. Yan, F. Weng, R. Ferraro, T. Kleespies, and H. Meng, "MiRS: An All-Weather 1DVAR Satellite Data Assimilation & Retrieval System," *IEEE Trans. Geosci. Remote Sens.*, vol. 49, no. 9, pp. 3249-3272, Sep. 2011.
- Figure 7c World View: https://worldview.earthdata.nasa.gov/